Phase Transitions Hot Paper

Deutsche Ausgabe: DOI: 10.1002/ange.201608530
Internationale Ausgabe: DOI: 10.1002/anie.201608530

High-Pressure Phase Transformations in $TiPO_4$: A Route to Pentacoordinated Phosphorus

Maxim Bykov, Elena Bykova, Michael Hanfland, Hanns-Peter Liermann, Reinhard K. Kremer, Robert Glaum, Leonid Dubrovinsky, and Sander van Smaalen*

Abstract: *Titanium(III) phosphate, $TiPO_4$, is a typical example of an oxyphosphorus compound containing covalent P–O bonds. Single-crystal X-ray diffraction studies of $TiPO_4$ reveal complex and unexpected structural and chemical behavior as a function of pressure at room temperature. A series of phase transitions lead to the high-pressure phase V, which is stable above 46 GPa and features an unusual oxygen coordination of the phosphorus atoms. $TiPO_4$-V is the first inorganic phosphorus-containing compound that exhibits fivefold coordination with oxygen. Up to the highest studied pressure of 56 GPa, $TiPO_4$-V coexists with $TiPO_4$-IV, which is less dense and might be kinetically stabilized. Above a pressure of about 6 GPa, $TiPO_4$-II is found to be an incommensurately modulated phase whereas a lock-in transition at about 7 GPa leads to $TiPO_4$-III with a fourfold superstructure compared to the structure of $TiPO_4$-I at ambient conditions. $TiPO_4$-II and $TiPO_4$-III are similar to the corresponding low-temperature incommensurate and commensurate magnetic phases and reflect the strong pressure dependence of the spin-Peierls interactions.*

The chemical element phosphorus plays a key role in the chemistry of life and many technological applications.[1] Phosphorus exhibits a rich chemistry forming thousands of compounds mainly with trivalent pyramidal ($\lambda^3\sigma^3$, where λ is the valence state, and σ is the coordination number) and pentavalent tetrahedrally coordinated ($\lambda^5\sigma^4$) compounds.[1] However, during the last decades, phosphorus compounds with alternative combinations of valence states and coordination schemes have also been discovered.[1] Oxyphosphorus compounds, which contain covalent P–O bonds (e.g., inorganic phosphates, phosphate esters, phosphoryl compounds), form the largest subset of phosphorus-containing compounds. In nature, phosphorus occurs almost exclusively in the pentavalent state as orthophosphate, a fact that reflects the high stability of the PO_4^{3-} anion. Any modifications of this stable $\lambda^5\sigma^4$ configuration require a large amount of energy. Therefore, all attempts to synthesize phosphorus compounds with σ^5 or σ^6 coordination have, thus far, mainly used organophosphorus precursors.[2,3]

Recent advances in diamond anvil cell (DAC) techniques combined with third-generation synchrotron facilities have meant that chemical reactions and phase transformations can be monitored by in situ X-ray diffraction up to ultrahigh pressures.[4–7] Experiments at high pressures have revealed unexpected chemistry and unusual stoichiometries of iron oxides and alkali halides.[8,9] In 2007, employing high-pressure techniques, the first observation of $\lambda^6\sigma^6$ phosphorus coordination was reported for berlinite, $AlPO_4$, at high pressures.[10] This study triggered systematic investigations towards the $\sigma^4\rightarrow\sigma^6$ transition in phosphates and related materials.[11–14] This information turned out to be essential for understanding the mechanisms of densification of widely used phosphorus oxide and oxynitride glasses.[15,16] In fact, the hunt for compounds with pentacoordinated phosphorus was initially driven by the expectation that σ^5-P may have unique catalytic properties. Yet, inorganic compounds containing phosphorus surrounded by five oxygen atoms have not been reported to date. It was predicted that σ^5 phosphorus may appear in compressed P_2O_5.[13] However, there is no experimental evidence for such a transformation. Herein, we report the first observation of an inorganic network structure where a phosphorus atom is coordinated by five oxygen atoms. This coordination is found in titanium(III) phosphate, $TiPO_4$, at pressures above 46 GPa.

$TiPO_4$ belongs to the family of MPO_4 (M = Ti, Tl, V, In) phosphates, which crystallize in the $CrVO_4$ structure type (space group *Cmcm*, with four formula units in the unit cell).[17,18] Under ambient conditions, the structure of $TiPO_4$ consists of edge-sharing TiO_6 octahedra forming infinite chains along the *c* axis. These chains are interconnected by oxygen atoms that belong to PO_4 tetrahedra (Figure 1). Theoretical calculations have predicted the following

[*] Dr. M. Bykov, Dr. E. Bykova, Prof. Dr. L. Dubrovinsky
Bayerisches Geoinstitut
University of Bayreuth
95440 Bayreuth (Germany)
E-mail: maxim.bykov@uni-bayreuth.de
Dr. M. Bykov, Prof. dr. S. van Smaalen
Laboratory of Crystallography
University of Bayreuth
95440 Bayreuth (Germany)
Dr. M. Bykov
Materials Modeling and Development Laboratory
National University of Science and Technology "MISIS"
119049 Moscow (Russia)
Dr. M. Hanfland
ESRF, 38000 Grenoble (France)
Dr. H.-P. Liermann
Deutsches Elektronen-Synchrotron (DESY)
22607 Hamburg (Germany)
Dr. R. K. Kremer
Max Planck Institute for Solid State Research
70569 Stuttgart (Germany)
Prof. Dr. R. Glaum
Institute of Inorganic Chemistry
University of Bonn, 53121 Bonn (Germany)
Supporting information and the ORCID identification number(s) for the author(s) of this article can be found under: http://dx.doi.org/10.1002/anie.201608530.

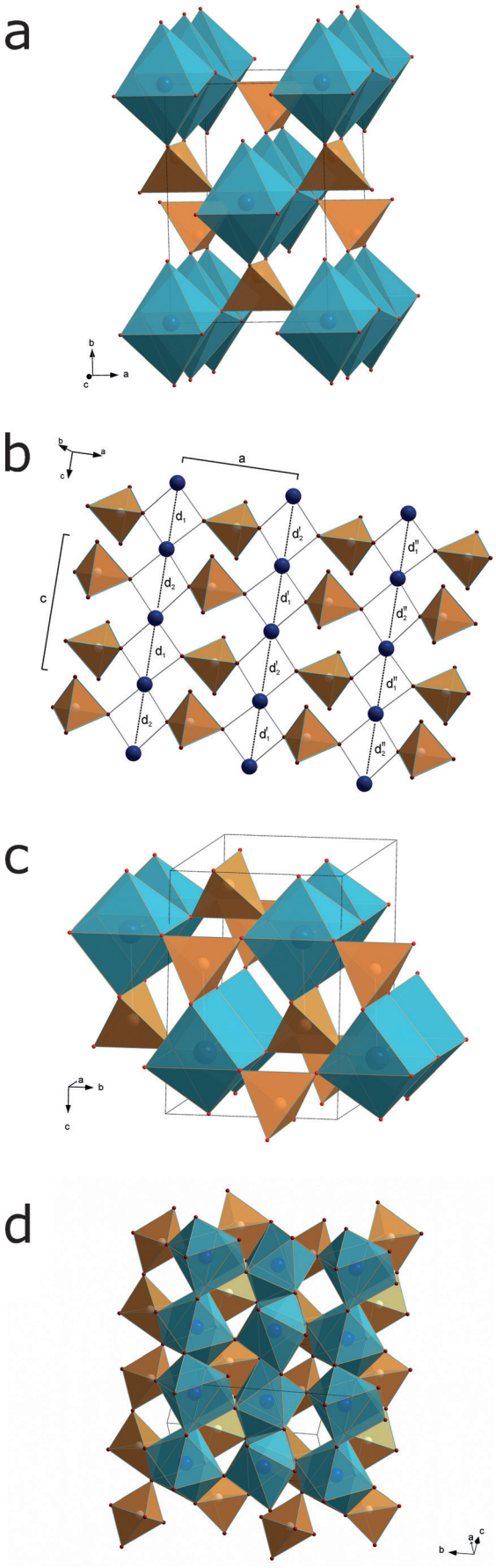

sequence of phase transitions in $TiPO_4$ upon an increase in pressure: *Cmcm*→zircon ($I4_1/amd$)→scheelite ($I4/a$)→wolframite ($P2/c$).[12] However, these transformations have never been experimentally verified. $TiPO_4$ is a peculiar member of the $CrVO_4$ structure family because of its low-dimensional magnetic properties. Upon cooling, it undergoes normal–incommensurate–commensurate phase transitions towards a dimerized spin-Peierls state.[19–21] The exchange interaction may be enhanced in spin-Peierls systems at high pressures,[22] which might lead to various magnetostructural transitions replacing the phase transitions predicted by classical crystal chemistry considerations.

We have characterized the high-pressure structural behavior of $TiPO_4$ by single-crystal X-ray diffraction on samples within DACs (see the Experimental Section for details). The ambient-pressure *Cmcm* phase (denoted as $TiPO_4$-I) is stable up to 4.5 GPa. Further compression leads to a phase transition, which was evidenced by the appearance of weak satellite reflections in the diffraction pattern. These reflections could be indexed on the basis of the unit cell of $TiPO_4$-I together with a modulation wave vector $\mathbf{q} = (\sigma_1, 0, 0)$ with $\sigma_1 = 0.558(3)$ at 6.0 GPa. We denoted this incommensurate phase as $TiPO_4$-II. Analysis of the diffraction symmetry and systematic absences revealed the superspace group $Cmcm(\sigma_1 00)0s0$ (No. 63.1.13.8 with the standard setting $Amam(00\sigma_3)0s0$).[23,24] The primary distortion involves the formation of Ti–Ti dimers within the Ti chains (Figure 1b). The displacements of the oxygen and phosphorus atoms follow those of the Ti atoms to minimize the internal strain within the structure.

A lock-in phase transition towards $TiPO_4$-III occurred between 6.0 and 7.3 GPa. The fourfold superstructure of $TiPO_4$-III can be described by the same superspace group as $TiPO_4$-II, but with $\sigma_1 = 0.5$. The rational value of σ_1 indicates that the structure can be alternatively described as a $2a \times b \times c$ supercell. Among the three possible 3D space groups (*Pmnm*, *Pbnm*, and $P2_1nm$) compatible with the superspace group, the best fit to the diffraction data was obtained for the $P2_1nm$ model (standard setting $Pmn2_1$, No. 31; see the Supporting Information). As for $TiPO_4$-II, the crystal structure of $TiPO_4$-III consists of dimerized chains of Ti atoms along the *c* axis. However, commensurability implies the presence of only two different kinds of chains instead of the infinite number of chains present in $TiPO_4$-II. Compression of $TiPO_4$-III up to 43 GPa provoked no further structural anomalies: The lattice parameters, unit cell volume, and average Ti–Ti distances smoothly decreased with pressure without any discontinuities (Figure 2a,b). A fit of the third-order Birch–Murnaghan equation of state to the experimental data resulted in a bulk

Figure 1. a) Crystal structure of $TiPO_4$ under ambient conditions. TiO_6 octahedra: light blue, PO_4 tetrahedra: orange. b) Incommensurate crystal structure of $TiPO_4$-II at 6.0 GPa. Each chain of Ti atoms (blue spheres) along the *c* axis is characterized by two Ti–Ti distances (d_1 and d_2). These distances are different for different chains ($d_1 \neq d_1' \neq d_1''$) along the *a* axis. The translational symmetry along the *a* axis is therefore lost. The Ti–Ti distances vary between 2.9348(8) and 3.1429(8) Å. c) Crystal structure of $TiPO_4$-IV at 48 GPa. d) Crystal structure of $TiPO_4$-V at 48 GPa.

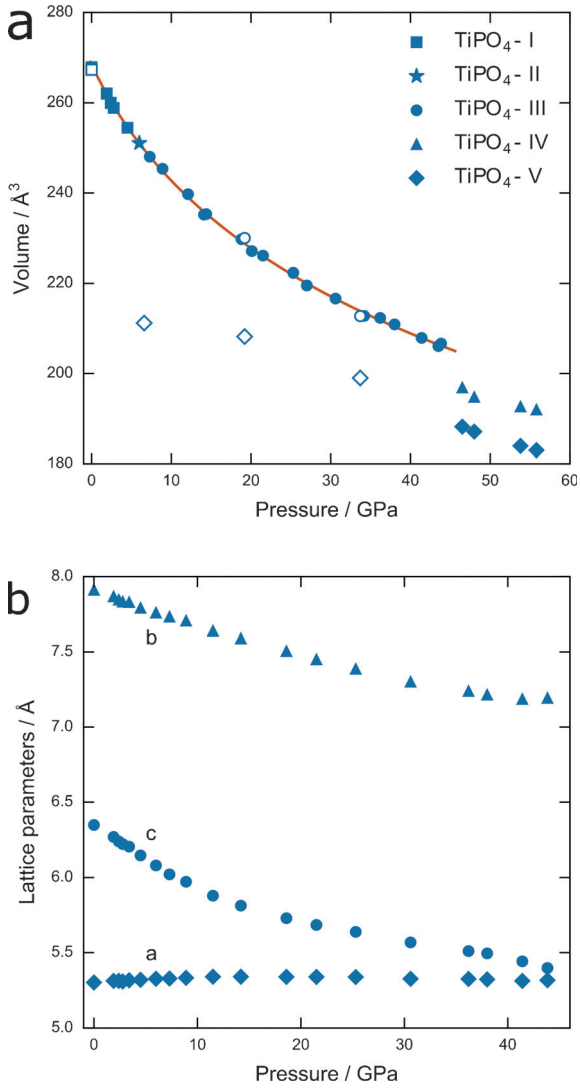

Figure 2. a) Pressure dependence of the unit cell volume of $TiPO_4$ in the $TiPO_4$-I, $TiPO_4$-II, and $TiPO_4$-III phases. For $TiPO_4$-II and $TiPO_4$-III, the volumes given are the volumes of the average structures. Open symbols correspond to the decompression experiment. The solid curve represents the fit of the third-order Birch–Murnaghan[29] equation of state to the experimental data. b) Pressure dependence of the lattice parameters of $TiPO_4$.

modulus $K_0 = 72(4)$ GPa and its pressure derivative $K_0' = 6.5$. These results are in a good agreement with previous theoretical calculations.[12] $TiPO_4$ is more compressible than known phosphates with scheelite, monazite, or zircon structures (APO_4, A = Sc, Lu, Yb, La, Nd, Eu, Gd, Er, Y)[25] and less compressible than $AlPO_4$[10] and $GaPO_4$,[26] which possess quartz-like and cristobalite-like structures, respectively. The compression of $TiPO_4$ is anisotropic, and its mechanism can be understood by analyzing the individual compressibilities of TiO_6 and PO_4 polyhedra (see the Supporting Information for details).[27]

$TiPO_4$-II is similar to the low-temperature incommensurate phase, and $TiPO_4$-III is similar to the low-temperature spin-Peierls (SP) phase, albeit with smaller unit-cell volumes.[19,20] The increase in the SP transition temperatures can be ascribed to the strong positive pressure dependence of the intrachain spin-exchange couplings. The temperature of the spin-Peierls transition (T_{SP}) is proportional to the ratio between intrachain and interchain spin-exchange interactions.[28] The large positive slope of the T_{SP} pressure dependence is due to the significant compressional anisotropy of $TiPO_4$ (Figure 2b). The most compressible direction in the crystal is that of the TiO_4 ribbon chains (along the *c* axis); as the pressure increases, the Ti–Ti distances decrease considerably. In contrast, the crystal is least compressible in the *a* direction. This means that the interchain Ti–Ti distances, and therefore the interchain spin-exchange interactions, are much less affected by pressure than intrachain interactions, which in turn leads to a substantial increase in T_{SP}.

The diffraction pattern of $TiPO_4$ changes considerably at 46 GPa. A thorough analysis revealed two systems of Bragg reflections that are not related to each other, neither by a symmetry operation nor by a transformation of the lattice parameters, suggesting that at these pressures, two polymorphs coexist. At 48 GPa, the polymorph $TiPO_4$-IV has monoclinic symmetry $P2_1/m$ with $a = 5.146$, $b = 5.321$, $c = 7.150$ Å, and $\beta = 110.21°$; the polymorph $TiPO_4$-V is also monoclinic, $P2_1/c$ with $a = 4.721$, $b = 7.051$, $c = 6.300$ Å, and $\beta = 116.87°$. The formation of both polymorphs is accompanied by pronounced decreases in volume of 4.2% for $TiPO_4$-IV and 8.0% for $TiPO_4$-V (Figure 2a). Detailed crystallographic information is summarized in the Supporting Information, Table S7.

$TiPO_4$-IV consists of TiO_7 trigonal prisms capped on a single rectangular face. They share their trigonal faces, thus forming infinite chains (Figure 1c). The coordination number of phosphorus remains four, and the TiO_7 prisms are interconnected by PO_4 groups. The volume collapse is related to the densification of the packing of the oxygen atoms; half of the square-packed oxygen layers rearrange to a denser hexagonal packing (Figure 3). This, in turn, leads to an effective increase in the coordination number of the Ti atoms. However, the structure still retains the Ti chains with alternating Ti–Ti distances of 2.460(6) and 2.696(6) Å at 48 GPa. Such short distances suggest that $TiPO_4$-IV may be in a Peierls-distorted state rather than in the spin-Peierls state, as previously described for TiOCl, for example, at pressures above 15 GPa.[22] Nevertheless, rigorous justification of this phenomenon requires further theoretical studies.

Compared to $TiPO_4$-IV, the formation of $TiPO_4$-V requires more significant atomic rearrangements. The structure of $TiPO_4$-V is composed of PO_5 trigonal bipyramids, which form chains along the [101] direction through shared apical oxygen atoms (O_a). The chains are interconnected with each other by Ti atoms, which are linked to the equatorial oxygen atoms (O_e) of the PO_5 groups, thus forming layers parallel to (10−1), such that the Ti atoms are confined between these layers (Figure 1d). In this way, the Ti atoms have highly distorted snub disphenoid coordination. The P–O_e distances in the PO_5 units are 1.536, 1.539, and 1.557 Å while the P–O_a distances are slightly longer at 1.662 and 1.707 Å. The O–O distances vary from 2.160 Å (for the shortest O_a–O_e distance) to 2.767 Å (for the longest O_e–O_e distance). The increase in the P–O distances compared to

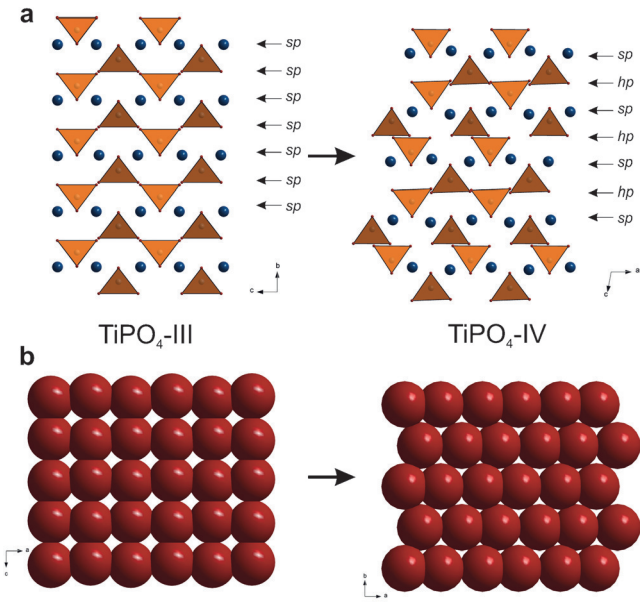

Figure 3. a) Schematic representation of the $TiPO_4$-III→$TiPO_4$-IV transformation. PO_4 tetrahedra: orange, Ti atoms: dark blue. $TiPO_4$-III contains only square-packed (sp) oxygen layers whereas $TiPO_4$-IV features both hexagonal-packed (hp) and sp layers. b) Square packing (left) and hexagonal packing of oxygen atoms in $TiPO_4$-III and $TiPO_4$-IV, respectively.

those in the PO_4 tetrahedra is in agreement with the increase in the coordination number of phosphorus. The Cambridge Structural Database (Nov. 2015)[30] contains 44 entries of molecular compounds comprising PO_5 trigonal bipyramids with mean P–O distances of 1.632 Å at ambient pressure, which is consistent with the average P–O distance in $TiPO_4$-V of 1.600 Å at 48 GPa.

The high-pressure behavior of ABO_4 compounds is usually estimated using a so-called Bastide's diagram,[31,32] based on the ionic radii r_A of cation A, r_B of cation B, and r_O of oxygen. The two-dimensional phase diagram is constructed on the basis of the ratios of the ionic radii, r_A/r_O and r_B/r_O. Each region of the diagram corresponds to a certain structure type. In the first approximation, both the r_A/r_O and r_B/r_O values increase with increasing pressure ("north-east rule"). In particular, for *Cmcm* phases, the expected high-pressure route is *Cmcm*→zircon ($I4_1/amd$)→scheelite ($I4/a$)→wolframite ($P2/c$).[12] Nevertheless, the experimental results clearly show different high-pressure structures. Both the Ti-σ^7-P-σ^4 and Ti-σ^8-P-σ^5 configurations, which correspond to $TiPO_4$-IV and $TiPO_4$-V, respectively, are apparently absent in the Bastide's diagram. This unprecedented transformation route can be explained by the enhanced stability of spin-Peierls-dimerized $TiPO_4$-III, which prevents the *Cmcm*→zircon phase transition, which had been predicted to occur at 12 GPa. Furthermore, the high kinetic barrier for reconstructive first-order transitions can also play a role in preventing the $TiPO_4$-III→scheelite or $TiPO_4$-III→wolframite transitions. The coexistence of $TiPO_4$-IV and $TiPO_4$-V is likely to be related to the kinetic hindrance of the formation of the $TiPO_4$-V phase. A similar phenomenon was observed in $BiPO_4$, where $BiPO_4$-III coexists with a monazite-type structure at high pressures.[33] The reverse transformation of $TiPO_4$-V upon pressure release is also hindered, as this phase can be quenched down to 6 GPa. Upon decompression, $TiPO_4$-IV disappeared at the same pressure where it had previously been formed, while we observed mixtures of $TiPO_4$-V with $TiPO_4$-III at 33.7 and 19.2 GPa, and with $TiPO_4$-II at 6.6 GPa. In the quenched sample, only TiPO4-I was observed. We would like to note that the volume data for $TiPO_4$-V may have become unreliable at 6.6 GPa and 19.2 GPa owing to the development of strain in this metastable phase.

In summary, fivefold phosphorus coordination has been known for molecular compounds.[1,34] Recently PN_5 trigonal bipyramids and tetragonal pyramids were found in $P_4N_6(NH)$[35] and γ-P_3N_5.[36] $TiPO_4$-V is the first example of PO_5 coordination in an inorganic compound. Our study demonstrates that the application of pressure may lead to novel types of phosphates and implies that other phosphates could have high-pressure polymorphs with pentacoordinated phosphorus.

Experimental Section

An initial single-crystal X-ray diffraction experiment was performed at the extreme-conditions beamline P02.2 of PETRAIII (DESY, Hamburg).[37,38] A preselected single crystal of $TiPO_4$ was placed into a BX90 DAC equipped with Boehler–Almax-type diamond anvils (250 μm culet diameter) along with ruby spheres for pressure determination. Neon was used as the pressure-transmitting medium. Data collection was performed as a series of ω scans with $\Delta\omega = 1°$/step at selected pressure points within the range 0–55.8 GPa both on compression and decompression. The diffraction intensities were collected with a PerkinElmer XRD 1621 flat-panel detector. The X-ray beam with a wavelength of 0.29 Å was focused with an array of compound refractive lenses to a size of 3×8 μm^2. The second experiment was performed at the beamline ID09A of the ESRF[39] (Grenoble, France), using the same crystal environment, a wavelength of 0.4104 Å, and a Mar555 flat-panel detector. The lattice parameters, components of the **q** vector, and the integrated intensities of the Bragg reflections were obtained from the measured images using the computer program CrysAlis^{Pro}. Bragg reflections overlapping with reflections from the diamonds or the pressure-transmitting medium were excluded from the data integration procedure. All structure refinements were performed with the JANA2006 crystallographic computing system.[40] All equation-of-state fits were performed with the EoSFit7c program using the third-order Birch–Murnaghan equation of state.[41] For details on the structure refinement, see the Supporting Information. The crystallographic information files (cif) may be obtained from FIZ Karlsruhe, 76344 Eggenstein-Leopoldshafen, Germany (fax: (+49)7247-808-666; e-mail: crysdata@fiz-karlsruhe.de), on quoting the deposition numbers CSD-431879-431891.

Acknowledgements

We thank the European Synchrotron Radiation Facility for the provision of synchrotron radiation facilities. Parts of this research were carried out at the light source PETRAIII at DESY, a member of the Helmholtz Association (HGF). Support through a grant from the Ministry of Education and Science of the Russian Federation (14.Y26.31.0005) is gratefully acknowledged. This research was supported by the DFG (Sm 55/15-2).

Keywords: high-pressure chemistry · phase transitions · phosphorus · spin-Peierls compounds · X-ray diffraction

How to cite: *Angew. Chem. Int. Ed.* **2016**, *55*, 15053–15057
Angew. Chem. **2016**, *128*, 15277–15281

[1] D. E. C. Corbridge, *Phosphorus: Chemistry, Biochemistry and Technology*, Taylor & Francis Group, Boca Raton, **2013**.
[2] K. C. K. Swamy, N. S. Kumar, *Acc. Chem. Res.* **2006**, *39*, 324–333.
[3] D. J. H. Smith in *Compr. Org. Chem.* (Eds.: D. Barton, W. D. Ollis), Pergamon, Oxford, **1979**.
[4] L. Dubrovinsky, *High Pressure Res.* **2013**, *33*, 451–452.
[5] F. J. Manjón, D. Errandonea, *Phys. Status Solidi* **2009**, *246*, 9–31.
[6] A. Katrusiak, *Acta Crystallogr. Sect. A* **2008**, *64*, 135–148.
[7] M. I. McMahon, *J. Synchrotron Radiat.* **2014**, *21*, 1077–1083.
[8] E. Bykova et al., *Nat. Commun.* **2016**, *7*, 10661.
[9] W. Zhang, A. R. Oganov, A. F. Goncharov, Q. Zhu, S. E. Boulfelfel, A. O. Lyakhov, E. Stavrou, M. Somayazulu, V. B. Prakapenka, Z. Konopkova, *Science* **2013**, *342*, 1502–1505.
[10] J. Pellicer-Porres, A. M. Saitta, A. Polian, J. P. Itié, M. Hanfland, *Nat. Mater.* **2007**, *6*, 698–702.
[11] D. Errandonea, O. Gomis, B. García-Domene, J. Pellicer-Porres, V. Katari, S. N. Achary, A. K. Tyagi, C. Popescu, *Inorg. Chem.* **2013**, *52*, 12790–12798.
[12] S. López-Moreno, D. Errandonea, *Phys. Rev. B* **2012**, *86*, 104112.
[13] M. A. Salvadó, P. Pertierra, *Inorg. Chem.* **2008**, *47*, 4884–4890.
[14] V. V. Brazhkin, J. Akola, Y. Katayama, S. Kohara, M. V. Kondrin, A. G. Lyapin, S. G. Lyapin, G. Tricot, O. F. Yagafarov, *J. Mater. Chem.* **2011**, *21*, 10442.
[15] M. R. Reidmeyer, M. Rajaram, D. E. Day, *J. Non-Cryst. Solids* **1986**, *85*, 186–203.
[16] V. V. Brazhkin, Y. Katayama, A. G. Lyapin, H. Saitoh, *Phys. Rev. B* **2014**, *89*, 104203.
[17] N. Kinomura, F. Muto, M. Koizumi, *J. Solid State Chem.* **1982**, *45*, 252–258.
[18] E. J. Baran, *J. Mater. Sci.* **1998**, *33*, 2479–2497.
[19] J. M. Law, C. Hoch, R. Glaum, I. Heinmaa, R. Stern, J. Kang, C. Lee, M.-H. Whangbo, R. K. Kremer, *Phys. Rev. B* **2011**, *83*, 180414.
[20] M. Bykov et al., *Phys. Rev. B* **2013**, *88*, 184420.
[21] D. Wulferding, A. Möller, K.-Y. Choi, Y. G. Pashkevich, R. Y. Babkin, K. V. Lamonova, P. Lemmens, J. M. Law, R. K. Kremer, R. Glaum, *Phys. Rev. B* **2013**, *88*, 205136.
[22] S. Blanco-Canosa, F. Rivadulla, A. Piñeiro, V. Pardo, D. Baldomir, D. Khomskii, M. Abd-Elmeguid, M. López-Quintela, J. Rivas, *Phys. Rev. Lett.* **2009**, *102*, 56406.
[23] H. T. Stokes, B. J. Campbell, S. van Smaalen, *Acta Crystallogr. Sect. A* **2011**, *67*, 45–55.
[24] S. van Smaalen, B. J. Campbell, H. T. Stokes, *Acta Crystallogr. Sect. A* **2013**, *69*, 1–16.
[25] R. Lacomba-Perales, D. Errandonea, Y. Meng, M. Bettinelli, *Phys. Rev. B* **2010**, *81*, 64113.
[26] L. C. Ming, Y. Nakamoto, S. Endo, C. H. Chio, S. K. Sharma, *J. Phys. Condens. Matter* **2007**, *19*, 425202.
[27] D. Errandonea, A. Muñoz, P. Rodríguez-Hernández, O. Gomis, S. N. Achary, C. Popescu, S. J. Patwe, A. K. Tyagi, *Inorg. Chem.* **2016**, *55*, 4958–4969.
[28] D. Fausti et al., *Phys. Rev. B* **2007**, *75*, 245114.
[29] F. Birch, *Phys. Rev.* **1947**, *71*, 809–824.
[30] F. H. Allen, *Acta Crystallogr. Sect. B* **2002**, *58*, 380–388.
[31] D. Errandonea, F. J. Manjón, *Prog. Mater. Sci.* **2008**, *53*, 711–773.
[32] J. P. Bastide, *J. Solid State Chem.* **1987**, *71*, 115–120.
[33] D. Errandonea, O. Gomis, D. Santamaría-Perez, B. García-Domene, A. Muñoz, P. Rodríguez-Hernández, S. N. Achary, A. K. Tyagi, C. Popescu, *J. Appl. Phys.* **2015**, *117*, 105902.
[34] C. M. Timperley, *Best Synthetic Methods: Organophosphorus(V) Chemistry*, Academic Press, London, **2015**.
[35] D. Baumann, W. Schnick, *Angew. Chem. Int. Ed.* **2014**, *53*, 14490–14493; *Angew. Chem.* **2014**, *126*, 14718–14721.
[36] K. Landskron, H. Huppertz, J. Senker, W. Schnick, *Angew. Chem. Int. Ed.* **2001**, *40*, 2643–2645; *Angew. Chem.* **2001**, *113*, 2713–2716.
[37] A. Rothkirch, G. D. Gatta, M. Meyer, S. Merkel, M. Merlini, H.-P. Liermann, *J. Synchrotron Radiat.* **2013**, *20*, 711–720.
[38] H.-P. Liermann et al., *J. Synchrotron Rad.* **2015**, *22*, 908–924.
[39] M. Merlini, M. Hanfland, *High Pressure Res.* **2013**, *33*, 511–522.
[40] V. Petricek, M. Dusek, L. Palatinus, *Z. Kristallogr.* **2014**, *229*, 345–352.
[41] R. J. Angel, M. Alvaro, J. Gonzalez-Platas, *Z. Kristallogr.* **2014**, *229*, 405–419.

Received: August 31, 2016
Revised: October 6, 2016
Published online: October 31, 2016

